ELSEVIER

Journal of Hydrology 260 (2002) 58–74

Journal of Hydrology

www.elsevier.com/locate/jhydrol

Screening model for volatile pollutants in dual porosity soils

Mohamed M. Hantush[a,*], Rao. S. Govindaraju[b], Miguel A. Mariño[c], Zhonglong Zhang[d]

[a]*Land Remediation and Pollution Control Division, National Risk Management Research Laboratory, ORD, USEPA, 26 West Martin Luther King Dr, Cincinnati, OH 45268, USA*

[b]*School of Civil Engineering, Purdue University, West Lafayette, IN 47907, USA*

[c]*Department of Land, Air and Water Resources, and Department of Civil and Environmental Engineering, University of California, Davis, CA 95616, USA*

[d]*Principal Environmental Systems Modeler, Concurrent Technologies Corporation, 510 Washington Avenue, Suite 120, Bremerton, WA 98337, USA*

Received 22 November 2000; revised 13 November 2001; accepted 26 November 2001

Abstract

This paper develops mass fraction models for transport and fate of agricultural pollutants in structured two-region soils. Mass fraction index models, based on a semi-infinite domain solution, are derived that describe leaching at depth, vapor losses through soil surface, absorption, and degradation in the dynamic- and stagnant-water soil regions. The models predict that leaching is the result of the combined effect of the upward vapor-phase transport relative to downward advection, residence time relative to half-life, dispersion, and lateral diffusive mass transfer. Simulations show that leached fraction of volatile compounds does not always decrease monotonically with increased residence time relative to the pollutant half-life, as a result of complex interactions among the different physical and biochemical processes. The results show that leaching, volatilization, and degradation losses can be affected significantly by lateral diffusive mass transfer into immobile-water regions and advection relative to dispersion (i.e. Peclet number) in the mobile-water regions. It is shown that solute diffusion into the immobile phase and subsequent biochemical decay reduces leaching and vapor losses through soil surface. Potential use of the modified leaching index for the screening of selected pesticides is illustrated for different soil textures and infiltration rates. The analysis may be useful to the management of pesticides and the design of landfills.

Keywords: Solute transport; Soil; Vapor transport; Pesticides; Screening models; Mobile–immobile phase; Biochemical decay; Adsorption; Dispersion; Mass transfer

1. Introduction

During the past 50 years, production of agricultural products (food and fiber) has intensified to meet consumer demands. The use of agricultural chemicals such as pesticides and nutrients has also increased dramatically during this period to improve agricultural efficiency and productivity. These chemicals are washed to surface waters by runoff and/or leached through the vadose zone to groundwater, thereby polluting the nation's waters and threatening human health as well as aquatic and terrestrial ecosystems. The cumulative effect of years of intensive agrichemical use has heightened public awareness of the often irreversible nature of nonpoint source pollution and the necessity to protect groundwater and surface water resources. This has pressured policy makers and regulatory agencies to implement management strategies to reduce the risk of ground-water contamination and

* Corresponding author.
E-mail address: hantush.mohamed@epa.gov (M.M. Hantush).

0022-1694/02/$ - see front matter
PII: S0022-1694(01)00597-2

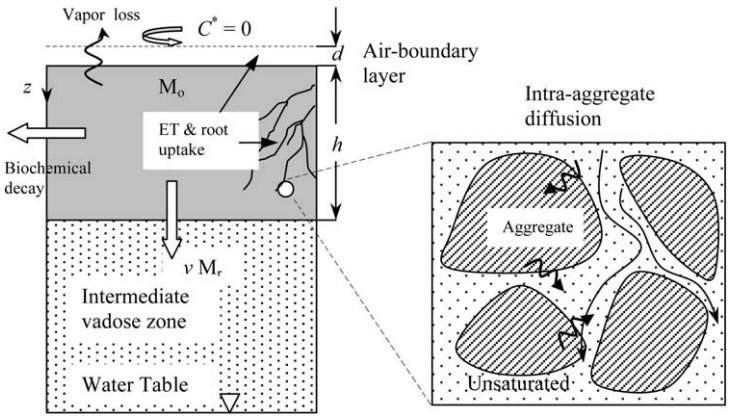

Fig. 1. Schematic illustration of pollutant loss pathways in two-region soils.

human and environmental exposure to toxic levels of the pollutants. Since groundwater contamination by nonpoint source pollutants is widespread, and often irreversible, and too complex and expensive to monitor regularly, cost-effective alternative approaches are needed. Scientists as well as regulatory agencies are increasingly relying on transport and fate models as tools to predict the behavior of pollutants in the environment, and to anticipate in advance potential pollution problems due to planned future developments. Such models have been used to predict the fate and exposure levels of pollutants along different exposure pathways in the environment (e.g. Wagenet and Rao, 1990; Jarvis, 1991).

This paper develops mass fraction models that describe the fate of pesticides as they move along different loss pathways in the subsurface from source to receptor locations. The models are not intended to simulate real-time concentrations, but rather to provide estimates for the likelihood of soil, air, and groundwater contamination. Simple index models were developed previously for screening organic chemicals relative to their mobility in the soil (Laskowski et al., 1982; Jury et al., 1984; Meeks and Dean, 1990). Leached fraction models are also used for screening of pesticides and estimating the likelihood of ground-water contamination (Rao et al., 1985; Meeks and Dean, 1990; van der Zee and Boesten, 1991; Beltman et al., 1995; Hantush et al., 2000). The advantage of these models over mobility index models is that they consider the interaction between the residence time in the soil and different loss and dispersing mechanisms on the likelihood of ground-water pollution by pesticides. Hantush et al. (2000) developed a leaching mass fraction index that lumps the effect of vapor losses through soil surface (volatilization) and lateral diffusive mass transfer into a single parameter. Although mass fraction models are not suitable for predicting concentrations, such as the more comprehensive PRZM (Carsel et al., 1985), LEACHM (Wagenet and Hutson, 1989) and MACRO (Jarvis, 1994) models, they nevertheless are suitable for screening purposes and regional-scale vulnerability assessment and require fewer input data generally available from the scientific literature and other sources. Kleveno et al. (1992) concluded that if sufficient data are available, the attenuation factor model (AF) (Rao et al., 1985) can be as effective as the dynamic PRZM model for screening and ranking pesticides. For the purpose of assessing relative ground-water vulnerability to pesticides, the use of complex numerical models is only justified when data are available at their level of complexity. This is even more challenging when dealing with nonpoint source pollutants at the watershed scale. Also, mass fraction models can be integrated with relative ease into a GIS framework to produce an effective tool for the assessment of soil and ground-water vulnerability to nonpoint source pollution in watersheds (e.g. Khan and Liang, 1989; Loague et al., 1995; Mulla et al., 1996; Shukla et al., 2000). However, models (e.g. index and mass fraction), however, are constrained by the uncertainty of model parameters associated with their spatial and

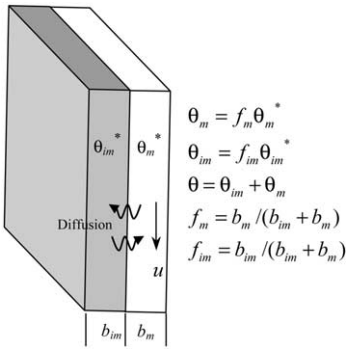

Fig. 2. Schematic illustration of a dual-porous slab model.

temporal variability and measurement errors. The impact of these uncertainties on the predictions of relative soil and ground-water vulnerability, or the likelihood for contamination, should be quantified for meaningful application to real field sites (e.g. Carsel et al., 1988; Loague et al., 1990, 1995, 1998; Freissinet et al., 1999; Diaz and Loague, 2000; Shukla et al., 2000).

When a pesticide is introduced into the soil surface, it follows different transport or loss pathways (Fig. 1). Part of the initially applied mass undergoes transformation into intermediate products called metabolites or completely degrades in the biologically active root zone. Some of the solute mass may be adsorbed onto the soil particulate surface and may undergo further degradation. Pesticides can partition into the vapor-phase and may then be transported by the mechanism of advection and/or gaseous diffusion within that gas-filled portion of the soil voids. Solutes diffuse laterally into soil regions occupied by stagnant waters (e.g. intra-aggregates) and may adsorb onto interior surfaces (i.e. absorption) and biodegrade therein. The solute is also available in soluble phase for uptake by the plant roots. Finally, a portion of the initially applied pesticide may leach below the vadose zone to groundwater by the mechanism of advection and dispersion.

In this paper, the impact of those processes on solute leaching to groundwater and vapor-phase emissions to the air is quantified. Expressions are derived for: (1) the leached fraction at depth in the soil; (2) the vapor loss fraction through soil–air interface; (3) the degraded fraction in the dynamic-water region (mobile-phase) of the soil profile; and (4) the degraded fraction in the stagnant-water region (immobile-phase) of the soil profile. Vapor loss at the soil surface by diffusion across an air boundary layer is treated more physically (Jury et al., 1991; Wagenet and Rao, 1990; Yates et al., 2000), as a boundary condition rather than being lumped into a first-order rate parameter (Hantush et al., 2000). The conditions under which the first-order approximation of volatilization losses is applicable will be investigated as a function of the Peclet number and the ratio of vapor loss rate to the advective flux, by comparison with a more physical model, which will be developed in this paper. The main advantage of the current development is that closed-form expressions are developed for the assessment of potential air pollution and the potential for biochemical decay of organic chemicals in soil. Specifically emphasized is the process of absorption, where a solute diffuses into stagnant-water pockets and sorbs onto the interior surfaces.

2. Theory

2.1. Transport in two-region soil

Transport of reactive solutes in a dual porosity medium (e.g. aggregated soil in Fig. 2) may be described by the following coupled system of equations for reactive constituents, Mobile phase:

$$R_{\mathrm{m}} \frac{\partial C_{\mathrm{m}}}{\partial t} + \beta R_{\mathrm{im}} \frac{\partial C_{\mathrm{im}}}{\partial t} + \beta k_{\mathrm{im}} R_{\mathrm{im}} C_{\mathrm{im}} = D_{\mathrm{m}} \frac{\partial^2 C_{\mathrm{m}}}{\partial z^2} - u \frac{\partial C_{\mathrm{m}}}{\partial z} - k_{\mathrm{m}}(1+\mu) R_{\mathrm{m}} C_{\mathrm{m}} \quad (1)$$

Immobile phase:

$$\beta R_{\mathrm{im}} \frac{\partial C_{\mathrm{im}}}{\partial t} + \beta k_{\mathrm{im}} R_{\mathrm{im}} C_{\mathrm{im}} = \alpha (C_{\mathrm{m}} - C_{\mathrm{im}}) \quad (2)$$

where

$$\mu = \frac{k_{\mathrm{u}}}{k_{\mathrm{m}} \theta_{\mathrm{m}} R_{\mathrm{m}}} \quad (3)$$

in which C_{m}, C_{im} are, respectively, resident solute concentrations in the mobile and immobile phases [M/L^3]; $u = v/\theta_{\mathrm{m}}$ is average pore-water velocity; v is soil water flux per unit area normal to flow direction [L/T]; $k_{\mathrm{m}} = \ln(2)/\lambda_{\mathrm{m}}$ and $k_{\mathrm{im}} = \ln(2)/\lambda_{\mathrm{im}}$ are, respectively, decay-rate constants in mobile and immobile phases [T^{-1}]; λ_{m}, λ_{im} are, respectively, solute

half-lives in mobile and immobile phases [T]; k_u is first-order rate of root uptake (passive uptake) [T^{-1}]; θ_m is volumetric mobile water content (per unit soil volume); α is rate mass transfer coefficient [T^{-1}]; β is fraction of immobile to mobile water content; $R_{im} = 1 + (f_{im}\rho_b K_d + \kappa^*_{im} K_H)/\theta^*_{im}$ is retardation factor in immobile water region; θ^*_m is volumetric immobile water content (per unit soil volume in immobile water region; i.e. phase averaged); κ^*_{im} is volumetric air content in immobile phase (per unit soil volume in immobile water region; i.e. phase averaged); f_{im} is fraction of soil in contact with immobile water; ρ_b is soil bulk density [M/L^3]; K_d is the distribution coefficient [L^3/M]; $R_m = 1 + (f_m\rho_b K_d + \kappa^*_m K_H)/\theta^*_m$ is retardation factor in mobile phase; θ^*_m is volumetric mobile water content (per unit soil volume in mobile water region; i.e. phase averaged); κ^*_{im} is volumetric air content in mobile phase (per unit soil volume in mobile water region; i.e. phase averaged); f_m is fraction of soil in contact with mobile water; and K_H is the dimensionless Henry's constant. The effective liquid-phase dispersion parameters are given by

$$D_m = \frac{\kappa^*_m}{\theta^*_m}\frac{(\kappa^*_m)^{10/3}}{n_m^2} D_g^a K_H + \alpha_l u + \frac{(\theta^*_m)^{10/3}}{n_m^2} D^* \quad (4)$$

$$D_{im} = \frac{\kappa^*_{im}}{\theta^*_{im}}\frac{(\kappa^*_{im})^{10/3}}{n_{im}^2} D_g^a K_H + \frac{(\theta^*_{im})^{10/3}}{n_{im}^2} D^* \quad (5)$$

where D_m is effective liquid-phase dispersion coefficient in mobile phase [L^2/T]; α_l is longitudinal dispersivity [L]; D_{im} is effective liquid-phase diffusion coefficient in immobile phase [L^2/T]; D_g^a is gaseous-phase diffusion coefficient [L^2/T]; D^* is liquid-phase diffusion coefficient [L^2/T]; and n_m and n_{im} are, respectively, porosities of the mobile and immobile phases. In Eqs. (4) and (5), the Millington and Quirk (1961) model is used to describe the soil gas and soil–liquid-phase diffusion coefficients.

The coupled system (1) and (2) extends the first-order rate transfer model to transport of reactive constituents with linear adsorption isotherms. By vertically averaging 3-D advective–dispersive transport equations in a dual-porous slab, as shown in Fig. 2; Hantush and Mariño (1998) derived the following expression for the mass rate transfer parameter:

$$\alpha = \frac{3\beta D_{im}}{b_{im}^2}\frac{\rho}{\beta + \rho} \quad (6)$$

$$\beta = \frac{\theta_{im}}{\theta_m} \quad (7)$$

$$\rho = \frac{t_{im}}{t_m},\ t_{im} = \frac{b_{im}^2}{D_{im}},\ t_m = \frac{b_m^2}{D_m} \quad (8)$$

in which ρ is the ratio of the diffusion time in immobile phase to that in mobile phase; θ_{im} the volumetric immobile water content (per unit soil volume) (Fig. 2); b_{im} the characteristic diffusion length in immobile water region [L] (e.g. average aggregate radius); and b_m is the characteristic diffusion length in mobile water region [L] (inter-aggregate pore radius). In most applications, the first-order rate model has been used to describe physical nonequilibrium transport by treating the coefficients α and β as calibration parameters (e.g. van Genuchten and Wierenga, 1976; Li et al., 1994; Griffioen et al., 1998). Expressions, however, have been developed that relate these parameters to the geometry of the immobile water zone, by fitting first-order rate transfer models with diffusion models of uniformly sized geometry (e.g. spherical, cylindrical, and finite slabs) (e.g. Parker and Valocchi, 1986; van Genuchten and Dalton, 1986). Although Eq. (6) is strictly applicable to infinite slabs of the immobile-phase region, it may be generalized to other geometries (e.g. spheres, cylinders, and finite slabs) by using appropriate shape factors of Parker and Valocchi (1986), van Genuchten and Dalton (1986), and Goltz and Roberts (1987).

The system of Eqs. (1), (2) and (6)–(8) has two distinct features: (1) it deals with reactive mobile–immobile phase transport in aggregated soils, and (2) the closed-form expression for the rate transfer coefficient α takes into account diffusion time in both phases. The significance of the latter will be illustrated in a numerical example herein. Implicit in the expressions of Parker and Valocchi (1986), van Genuchten and Dalton (1986), and Goltz and Roberts (1987) is that the diffusion time in the mobile phase is much smaller than that in the immobile phase, which is equivalent to setting $\rho \to \infty$ in Eq. (3) (Hantush and Mariño, 1998). This requires that $\rho \gg \beta$, which may not always be satisfied for highly volatile compounds, where D_m and D_{im} may be dominated by vapor-phase diffusion, and where the diffusion time in both the mobile and immobile phases may be of the same order of magnitude. To illustrate this quantitatively,

we consider a highly volatile compound (i.e. with a relatively high K_H) and substitute Eqs. (4) and (5) into Eq. (8); then, after neglecting the liquid-phase dispersion one obtains

$$\rho \approx \beta \frac{f_{im}}{f_m}\left(\frac{n_{im}}{n_m}\right)^2\left(\frac{1-\theta_m^*}{1-\theta_{im}^*}\right)^{13/3} \tag{9a}$$

where $f_{im}/f_m \approx b_{im}/b_m$. As an example illustration, consider the data: $n_{im} = 0.2$, $n_m = 0.25$, $\theta_{im}^* = 0.15$, $\theta_m^* = 0.2$, and $f_{im}/f_m \approx 2$. Inserting these values into Eq. (9a) yields $\rho/\beta \approx 2(0.2/0.25)^2(0.80/0.85)^{13/3} = 0.98$, which does not satisfy the condition $\rho \gg \beta$.

If we consider the specific case of purely diffusive transfer in a two-region immobile phase ($v = 0$) of nonvolatile compounds ($K_H \approx 0$), then

$$\rho \approx \beta \frac{f_{im}}{f_m}\left(\frac{n_{im}}{n_m}\right)^2\left(\frac{\theta_m^*}{\theta_{im}^*}\right)^{13/3}, \tag{9b}$$

and for the example data above: $\rho/\beta \approx 2(0.2/0.25)2(0.2/0.15)^{13/3} = 4.4$; i.e. the diffusion time is of the same order of magnitude in both phases, a condition which also may not be sufficient for ρ much larger than β. Of course, in this specific case the notion of mobile–immobile phase is irrelevant since transport is predominantly diffusive in both regions (e.g. inter-aggregate and intra-aggregate).

In Section 2.2, expressions will be developed for leaching of solutes in soils, vapor losses through soil surface, and biochemical decay in mobile–immobile phase soil profile.

2.2. Leaching in soil

In this section, we present closed-form expressions that describe leaching and transformation of organic chemicals as they partition into the vapor-phase and adsorbed phase in a dual porosity (e.g. aggregated) soil. The following assumptions are made: (1) the soil is composed of a structured dynamic water (mobile-phase) and stagnant water (immobile-phase) regions; (2) uniform and steady-state flow rate in the soil; (3) linear equilibrium partitioning isotherms; (4) vapor transport is diffusive and loss occurs in the mobile phase from the soil surface through an air boundary layer of thickness d (Fig. 1); and (5) root uptake can be described by a first-order rate process.

The following are the initial and boundary conditions

$$C_{im}(z,0), \quad C_m(z,0) = 0 \tag{10a}$$

$$F_g(0,t) = -\kappa_m D_g^s \frac{\partial C_g(0,t)}{\partial z} = -D_g^a \frac{C_g(0,t) - C^*}{d} \tag{10b}$$

$$F_l(0,t) = -\theta_m D_l \frac{\partial C_m(0,t)}{\partial z} + vC_m(0,t) = M_o\delta(t) \tag{10c}$$

$$C_{im}(\infty,t), \quad C_m(\infty,t) = 0 \tag{10d}$$

in which $C_g(z,t)$ is solute vapor concentration [ML^{-3}]; C^* is concentration of solute vapor above air-boundary layer, which is assumed to be zero in this analysis [ML^{-3}]; $\kappa_{im} = f_{im}\kappa_{im}^*$ is volumetric air content in immobile-water region (per unit soil volume); D is mobile phase soil dispersion, which is the sum of the second and third terms on the right-hand side of (4) [L^2/T]; M_o is chemical mass applied per unit area; and d is air-boundary layer, for a bare surface may be equal to 5 mm (Jury et al., 1991). The total solute flux through soil in mobile phase at any depth is the sum of advective–dispersive liquid-phase and diffusive vapor-phase fluxes, $F_m(z,t) = F_l(z,t) + F_g(z,t)$, and is given by

$$F_m(z,t) = -\theta_m D_m \frac{\partial C_m(z,t)}{\partial z} + vC_m(z,t) \tag{11}$$

$F_g(z,t)$ is solute vapor-phase flux [$ML^{-2}T^{-1}$] and $F_l(z,t)$ is solution phase flux [$ML^{-2}T^{-1}$]. If we use Henry's law to describe liquid-vapor partitioning,

$$C_g(z,t) = K_H C_m(z,t) \tag{12}$$

and substitute the right side of Eq. (12) into Eq. (10b), then the total solute flux at the soil surface (11) evaluated at $z = 0$, can be shown to be

$$F_m(0,t) = -\sigma[C_m(0,t) - (C^*/K_H)] + M_o\delta(t) \tag{13}$$

where

$$\sigma = \frac{K_H D_g^a}{d} \tag{14}$$

The mass applied per unit area, M_o, can be estimated based on two different scenarios of: (1) planned application, and (2) flushing of an initially contaminated

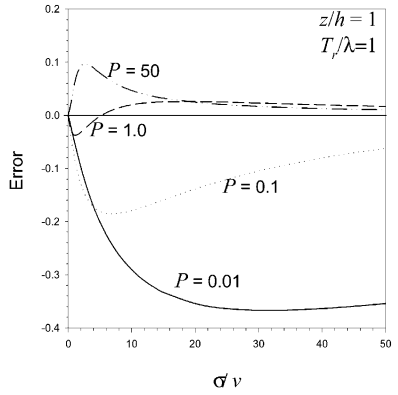

Fig. 3. Errors in leached fractions estimated from the first-order volatilization rate model of Hantush et al. (2000) and the modified expression (17).

surface layer. In the first mode, if the solute is introduced by aerial spraying (or sprinkler irrigation) at concentration C_0 at a rate q [$L^3/T/L^2$] during a time period Δt, we have $M_o = q\Delta t C_0$. In the second mode, if the soil is initially wet at θ_0 and contaminated with a uniform concentration C_0 to a depth L (fraction of centimeters below the soil surface), then $M_o = \theta_0 L C_0$. In both cases, leaching at depth will occur at a time scale much greater than Δt or the time required to completely flush the solute from the shallow depth of incorporation, for the Dirac-delta representation of the flux in Eq. (10c) to be a valid approximation.

We consider M_o to be the only source of solute and that $C^* = 0$. The leaching potential here is defined as the fraction of M_o that will eventually pass depth z, $I_l(z)$,

$$I_l(z) = (1/M_o)\int_0^\infty F_m(z,\tau)\mathrm{d}\tau \tag{15}$$

which can be rewritten in the form

$$I_l(z) = (1/M_o)\lim_{t\to\infty}\left\{\int_0^t F_m(z,\tau)\mathrm{d}\tau\right\} \tag{16}$$

The evaluation of Eq. (16) is carried out in the Appendix A to yield

$$I_l(z) = \frac{1+\xi^*}{2(\sigma/v)+1+\xi^*}\exp\left\{-\frac{P}{2}(\xi^*-1)\frac{z}{h}\right\} \tag{17}$$

where

$$\xi^* = \sqrt{1+4\frac{\ln(2)}{P}\frac{T_r}{\lambda_m}(1+\mu+\phi)} \tag{18}$$

and

$$\phi = \frac{\beta\alpha}{\beta k_{im}R_{im}+\alpha}\frac{R_{im}k_{im}}{R_m k_m} \tag{19}$$

in which $P = hu/D_m$ is a Peclet number and $T_r = hR_m/u$ is apparent residence time [T].

Eq. (17) is a modification to the expression obtained by Hantush et al. (2000): $I_l(z) = \exp\{-P/2(\xi^*-1)z/h\}$, $\mu = (k_u + \sigma/h)/(k_m\theta_m R_m)$. In the latter, vapor loss from the soil surface was approximated by a first-order rate process and, in effect, was lumped into the parameter, μ, to account for the combined effect of volatilization and root uptake. In this paper, however, μ accounts for root uptake only. The expression given by Eq. (17) is more physically based than the first-order approximation of vapor losses whose validity may be limited to small values of σ/v, where the downward advective flux by infiltration is occurring at a rate higher than the upward vapor flux (i.e. volatilization through soil surface). The difference between Eq. (17) ($T_r/\lambda = 1$ and $z/h = 1$) and Hantush et al. (2000) model, in which volatilization is approximated by a first-order rate process, is shown in Fig. 3 (e.g. an error of -0.4 is equivalent to an absolute error of 40%). In general, the error increases significantly when $P < 1$ (e.g. highly volatile compounds) over a wide range of σ/v. In this case ($T_r/\lambda = 1$ and $z/h = 1$) leaching errors committed by first-order approximation of volatilization losses appear to be less than 10% for $\sigma/v < 1$, and less than 20% for all values of σ/v when $P > 0.1$. The error is significant and can be greater than 30% for $\sigma/v > 10$ when $P \le 0.01$.

2.3. Vapor loss from soil surface

The fraction of M_o that constitutes vapor loss through soil surface is obtained by integrating the vapor flux at the soil–air interface in time,

$$I_v = \lim_{t\to\infty}\left\{-(1/M_o)\int_0^t F_g(0,\tau)\mathrm{d}\tau\right\}$$
$$= \lim_{t\to\infty}\left\{(\sigma/M_o)\int_0^t C_m(0,\tau)\mathrm{d}\tau\right\} \tag{20}$$

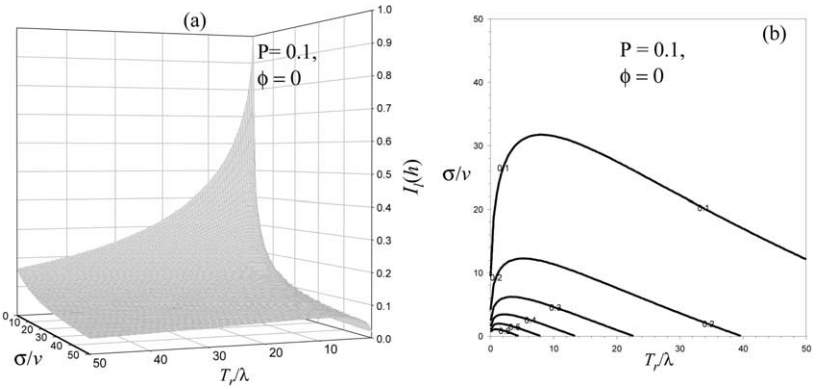

Fig. 4. Leaching at depth $z = h$ as a function of T_r/λ and σ/v with $P = 0.1$ and $\phi = 0$: (a) 3-D plot, and (b) contour plot.

Thus, by applying the Laplace identity (A13), we have

$$I_v = (\sigma/M_o)\lim_{p\to 0}\tilde{C}_m(0;p) \tag{21}$$

in which $\tilde{C}_m(0;p)$ is the laplace transform of $C_m(0,t)$. By substituting $z = 0$ and $C^* = 0$ in Eq. (A8) and the resulting equation with Eq. (A10) into Eq. (21) and carrying on the limit, one obtains:

$$I_v = \frac{2(\sigma/v)}{2(\sigma/v) + 1 + \xi^*} \tag{22}$$

As $\sigma/v \to 0$, $I_v \to 0$, and as $\sigma/v \to \infty$, $I_v \to 1$. Thus, significant losses from soil surface are predicted by the model for highly volatile pesticides (with relatively large K_H). Eq. (22) provides an estimate of the pesticide's mass per unit area available in the vapor-phase for transport by air or for foliar uptake (e.g. van der Werf, 1996). The latter may contribute more than root uptake to plant residues, which constitutes an important exposure pathway to humans and animals.

2.4. Losses in mobile phase

Fraction of M_o lost by biochemical decay in the mobile phase from a soil profile of depth h is given by

$$I_m(h) = \lim_{t\to\infty}\left\{(1/M_o)\int_0^t\int_0^h \theta_m k_m R_m C_m(z,t)\mathrm{d}z\,\mathrm{d}t\right\} \tag{23}$$

By employing the Laplace identity (A13), we have

$$I_m(h) = \theta_m k_m R_m(1/M_o)\lim_{p\to 0}\left\{\int_0^h \tilde{C}_m(z;p)\mathrm{d}z\right\} \tag{24}$$

in which $\tilde{C}_m(z;p)$ is the laplace transform of $C_m(z,t)$. The integral is carried out by substituting Eqs. (A9) and (A10) into Eq. (A8) and the resulting expression into Eq. (24), followed by taking the limit $p \to 0$, and integrating with respect to z, to yield

$$I_m(h) = \frac{1}{1+\phi}\,\frac{1+\xi^*}{2(\sigma/v)+1+\xi^*}\left(1 - \mathrm{e}^{-(P/2)(\xi^*-1)}\right) \tag{25}$$

2.5. Losses in immobile phase

Losses in the immobile-water zone by degradation within depth h can be expressed as

$$I_{im}(h) = \lim_{t\to\infty}\left\{(1/M_o)\int_0^t\int_0^h \theta_m\alpha\left[C_m(z,\tau) - C_{im}(z,\tau)\right]\mathrm{d}z\,\mathrm{d}t\right\} \tag{26}$$

Similarly, by applying Eq. (A13), Eq. (26) can be rewritten as

$$I_{im}(h) = (1/M_o)\theta_m\alpha\lim_{p\to 0}\left\{\int_0^h [\tilde{C}_m(z;p) - \tilde{C}_{im}(z;p)]\mathrm{d}z\right\} \tag{27}$$

The substitution of Eq. (A6) for $\tilde{C}_{im}(z;p)$ in Eqs. (27)

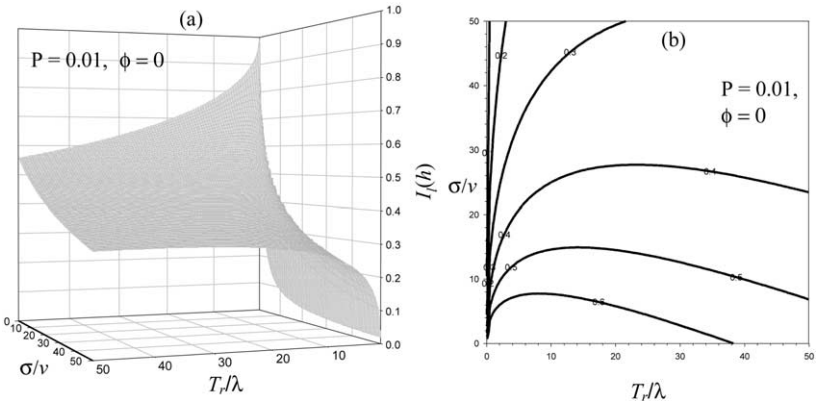

Fig. 5. Leaching at depth $z = h$ as a function of T_r/λ and σ/v with $P = 0.01$ and $\phi = 0$: (a) 3-D plot, and (b) contour plot.

and (A8) for $\tilde{C}_m(z;p)$with Eqs. (A9)–(A10), and taking the limit $p \to 0$, after carrying out the integration, yields

$$I_{im}(h) = \frac{\phi}{1+\phi}\frac{1+\xi^*}{2(\sigma/v)+1+\xi^*}(1 - e^{-(P/2)(\xi^*-1)}) \tag{28}$$

This equation describes the fraction of mass per unit area that undergoes absorption and subsequent transformation in the immobile phase.

The total losses in the soil profile due to biochemical degradation are the sum of Eqs. (25) and (28), $I_m(h) + I_{im}(h)$,

$$I_{deg}(h) = \frac{1+\xi^*}{2(\sigma/v)+1+\xi^*}(1 - e^{-(P/2)(\xi^*-1)}) \tag{29}$$

The following mass balance can be verified

$$I_l(h) + I_v(h) + I_{deg}(h) = 1 \tag{30}$$

Eq. (29) provides an estimate to the fraction of mass per unit area that is potentially available for transport as metabolites below soil depth h.

3. Results and discussion

Hereinafter, we assume ($\lambda_{im} = \lambda_m = \lambda$, where λ is solute half-life in both mobile–immobile phases. Figs. 4–6 display 3-D variations of leached fraction $I_l(h)$ as a function of the dimensionless variables T_r/λ and σ/v, for different values of P and ϕ. At $\sigma/v = 0$, leached fraction decreases monotonically with T_r/λ, while as σ/v becomes larger than zero, an optimal leached

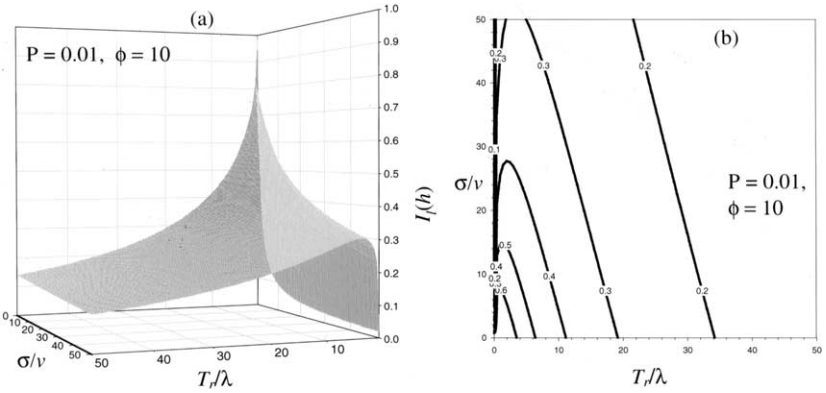

Fig. 6. Leaching at depth $z = h$ as a function of T_r/λ and σ/v with $P = 0.01$ and $\phi = 10$: (a) 3-D plot, and (b) contour plot.

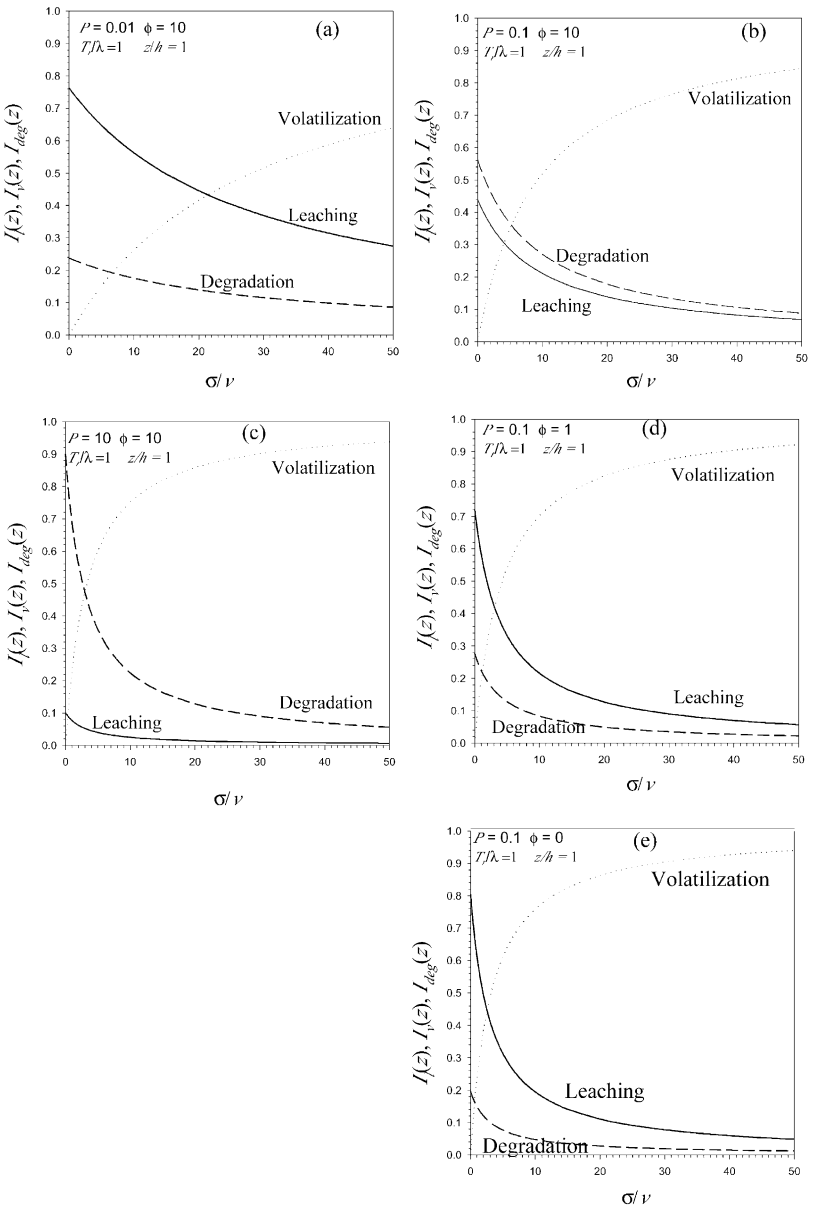

Fig. 7. Leached, biodegraded, and volatilized fractions at $z = h$ and $T_r/\lambda = 1$ as a function of σ/v: (a) $P = 0.01$ and $\phi = 10$, (b) $P = 0.1$ and $\phi = 10$, (c) $P = 10$ and $\phi = 10$, (d) $P = 0.1$ and $\phi = 1$, and (e) $P = 0.1$ and $\phi = 0$.

fraction develops at a given value of T_r/λ, as Figs. 4–6 show. As the latter becomes larger than zero, the increased residence time relative to pesticide's half-life favors greater transformation losses and therefore reduced solute concentration. This reduces vapor loss through soil surface significantly, since it is directly proportional to solution concentrations (by Henry's law) and assuming moisture content unchanged, thereby increasing leached fractions. The combined effect of increased residence time relative to half-life and decreased vapor losses from soil surface on leached fractions depends on the relative magnitude

Table 1
Representative soil physical properties

Soil texture	ρ_b (Kg/m^3)	f_{om} (%)[a]	f_{oc} fraction[b]	θ_s[c]	b[c]	K_s[c] (cm/min)
Sand	1625[d]	0.71	0.004118	0.395	4.05	1.056
Loamy sand	1500[e]	0.61	0.003538	0.41	4.38	0.938
Sandy loam	1300[d]	0.71	0.004118	0.435	4.90	0.208
Silt loam	1470[d]	0.58	0.003364	0.485	5.30	0.0432
Loam	1400[e]	0.52	0.003016	0.451	5.39	0.0417
Sandy clay loam	1370[e]	0.19	0.001102	0.42	7.12	0.0378
Silty clay loam	1340[e]	0.13	0.000754	0.477	7.75	0.0102
Clay loam	1280[d]	0.10	0.00058	0.476	8.52	0.0147
Sandy clay	1280[e]	0.38	0.002204	0.426	10.40	0.0130
Silt clay	1260[e]	0.38[e]	0.002204	0.492	10.40	0.0062
Clay	1200[e]	0.38	0.002204	0.482	11.40	0.0077

[a] From Rawls (1983).
[b] $f_{oc} = f_{om}/1.724$.
[c] From Li et al. (1976).
[d] Average values from Jury (1986).
[e] Assumed.

of these two opposing effects. van der Zee and Boesten (1991) described a similar phenomenon to account for the impact of longer residence time and smaller crop uptake on the leached fraction. For smaller values of T_r/λ the decreased vapor losses from soil surface (or volatilization loss) dominate, leading to increased leaching. For larger T_r/λ the increased residence time relative to half-life favors greater transformation losses that dominate and results in decreasing leaching. Figs. 4 and 5 show that solute dispersion in the dynamic phase increases leached fraction considerably over the range of values of T_r/λ and σ/v, when P becomes smaller (e.g. Beltman et al., 1995).

Comparison of Fig. 5(a) with Fig. 6(a) indicates that for small T_r/λ leaching is greater for $\phi = 10$ than for $\phi = 0$ at $\sigma/v = 50$, but smaller at larger T_r/λ values. This is because diffusive mass transfer into stagnant-water zones, as a lateral dispersive process, reduces solute concentrations. This affects both transformation and vapor loss, which are reduced considerably, thereby leading to greater leached fractions for increasing but small T_r/λ. Fig. 6(a) and (b) show that for larger ϕ, variations of leached fraction with σ/v diminishes for larger T_r/λ.

Fig. 7 shows leached fraction at $z = h$ and $T_r/\lambda = 1$, volatilization losses (or vapor loss from soil surface), and transformation (biochemical) losses as a function of the dimensionless variable σ/v for different values of P and ϕ. Volatilization loss, I_v, show relatively greater variations with P than ϕ at $T_r/\lambda = 1$. When P increases, dispersion in the mobile phase becomes smaller relative to advection, and vapor loss from soil surface increases due to increased concentration gradients at the interface. Dispersion enhances leaching and as a result reduces concentrations at the soil surface (e.g. van der Zee and Boesten, 1991; Beltman et al., 1995; Hantush et al., 2000). Lateral dispersion produced by diffusion into stagnant-water regions and subsequent degradation is another mechanism that may reduce concentration gradient across the soil–air interface, thereby leading to decreased volatilization losses. The effect of the immobile-water phase (ϕ) on I_v, however, appears to be less profound than that of dispersion, as comparisons among Fig. 7(b), (d), and (e) indicate.

Whereas in Fig. 7(b)–(e) I_v shows a sharp increase with $\sigma/v \leq 20$, the combined effect of dispersion in the mobile water region and lateral diffusion and mixing in the immobile phase is to moderate volatilization losses, as illustrated by the gradual increase of I_v with σ/v in Fig. 7(a). Comparisons among Fig. 7(a)–(c) show that a smaller P favors greater losses at depth $z = h$ by leaching than by degradation at $T_r/\lambda = 1$. The opposite, however, may be true when P is greater than 0.1, where degradation dominates both leaching for all values of σ/v and volatilization losses for small values of σ/v. It is evident from Fig. 7(a) that $P = 0.01$ is the most favorable scenario for

Table 2
Chemical properties

Chemical	K_{oc} (m^3/kg)	K_H	λ (days)
Atrazine	1.60×10^{-1}	2.50×10^{-7}	71
Aldicarb	1.00×10^{-2}	1.00×10^{-4}	28
Bromacil	7.20×10^{-2}	3.70×10^{-8}	350
Captan	3.30×10^{-2}	4.90×10^{-5}	3
Carbaryl	2.29×10^{-1}	1.40×10^{-3}	22
Carbofuran	2.80×10^{-2}	3.10×10^{-7}	40
Chlordane	3.80×10^{1}	2.20×10^{-4}	3500
Chloropyrifos	6.07	1.80×10^{-4}	63
Cyanazine	1.68×10^{-1}	1.20×10^{-4}	108
2,4-D	2.00×10^{-2}	5.60×10^{-9}	15
DDT[a]	2.40×10^{2}	2.00×10^{-3}	3837
Diazinon	8.50×10^{-2}	5.00×10^{-5}	32
Dieldrin	1.20×10^{1}	6.70×10^{-4}	868
Diuron	3.80×10^{-1}	5.40×10^{-8}	328
EDB	4.40×10^{-2}	3.50×10^{-2}	3650
EPTC	2.80×10^{-1}	5.90×10^{-4}	30
Ethoprophos	1.20×10^{-1}	6.00×10^{-6}	50
Heptachlor	2.40×10^{1}	1.45×10^{-1}	2000
Lindane	1.3	1.30×10^{-4}	266
Linuron	8.60×10^{-1}	2.50×10^{-6}	75
Mehyl bromide	2.20×10^{-2}	1.5	55
Methyl parathion	5.1	4.40×10^{-6}	15
Monuron	1.80×10^{-1}	7.60×10^{-9}	166
Napropamide	3.00×10^{-1}	7.90×10^{-7}	70
Parathion	1.10×10^{1}	6.10×10^{-6}	18
Pentachlorphenol	1.43×10^{1}	8.80×10^{-2}	48
Phorate	6.60×10^{-1}	3.10×10^{-4}	82
Picloram	2.60×10^{-2}	1.90×10^{-8}	138
Prometryne	6.10×10^{-1}	5.60×10^{-7}	60
Simazine	1.40×10^{-1}	3.40×10^{-8}	75
Triallate	3.6	7.90×10^{-4}	100
Trifluralin	7.3	6.70×10^{-3}	132

[a] Jury et al. (1991).

ground-water pollution due to greater dispersion, even though $\phi = 10$. Note that the leached fraction is greater than 30% of the initial mass at $\sigma/v \le 50$. With the exception of Fig. 7(a), volatilization losses are estimated to be at least 10% at $\sigma/v = 1$, and become considerably larger at greater σ/v values. Fig. 7(b), (d), and (e) show that losses by leaching and volatilization generally decrease with increasing ϕ. However, leached fractions are almost invariant with ϕ at large values of σ/v. Degradation increases significantly with ϕ over the range of values of σ/v.

Eqs. (17), (22), (25), (28), and (29) can be applied to a stratified soil profile. For example, leaching from a soil profile made up of four distinct layers is equal to the product $\prod_{i=1}^{i=4} I_l^i$, in which I_l^i is the leached fraction from layer i. Such sequential application of the relationships to a layered soil, however, assumes that layer interactions have no significant effect on transport as implied by the semi-infinite boundary condition (10d). Barry and Parker (1987), using moment analysis, showed that a semi-infinite solution will closely approximate transport in a finite soil length for $P > 16$ (see also, Parlange and Starr, 1978).

4. Application to screening of pesticides

Tables 1 and 2 show, respectively, soil physical characteristics according to texture and chemical properties of selected pesticides (Rao et al., 1985). Tables 3 and 4 show a listing of pesticides whose leached fraction below depth $z = h = 1$ m do not exceed 1% (i.e. $I_l < 0.01$) for infiltration rates $v =$ 0.01, 0.1, and 1.0 m/d. This is equivalent to 99% attenuation of the mass introduced. The following data are used: $\alpha_l = 1$ cm, $\mu = 0$, and $D_g^a = 0.432\ m^2$/d. Flow is approximated by gravity drainage; i.e. $v = K(\theta)$, from which θ is calculated from Campbell (1974) moisture characteristic model:

$$\theta = \theta_s\left(\frac{v}{K_s}\right)^{1/(2b+3)} \tag{31}$$

where $\theta = \theta_s$ if $v \ge K_s$. The screening results in the tables are based on the leached fractions relationship (17) and the purely convective-reactive limit of this equation (i.e. $P \to \infty$):

$$I_l(z) = \frac{v}{v+\sigma}\exp\left\{-\ln(2)\frac{T_r}{\lambda_m}(1+\mu+\phi)\right\}\frac{z}{h} \tag{32}$$

Pesticides that are marked with $*$ pass the convective screening test (i.e. $I_l \le 0.01$, I_l given by Eq. (32)), but fail the dispersive screening model (i.e. $I_l > 0.01$, I_l given by Eq. (17)) at depth 1 m.

Methyl bromide is the only chemical that passed the screening test in all soil textures for the chosen soil flux rates. It is highly volatile ($K_H = 1.5$) and relatively short-lived ($\lambda = 55$ d). Heptachlor satisfies the above leaching criterion in all soil textures at $v =$ 0.01 and 0.1 m/d, and in silty clay and clay soils, only at $v = 1.0$ m/d. Although this pesticide is resistive to biochemical decay ($\lambda = 2000$ d), it is volatile and highly adsorptive ($K_H = 0.145$, $K_{oc} = 24\ m^3$/Kg).

Table 3
List of chemicals satisfying 1% leaching criterion

	Sand	Loamy sand	Sandy loam	Silt loam	Loam	Sandy clay loam
$v = 0.01$ m/d	Captan Carbaryl Chlordane Chloropyrifos DDT Dieldrin EDB EPTC Heptachlor Linuron Methyl bromide Methyl parathion Parathion Pentachlorphenol Phorate Prometryne Triallate Trifluralin	Captan Carbaryl Chlordane Chloropyrifos DDT Dieldrin EDB EPTC Heptachlor Methyl bromide Methyl parathion Parathion Pentachlorphenol Triallate Trifluralin	Captan Carbaryl Chlordane Chloropyrifos DDT Dieldrin EDB EPTC Heptachlor Methyl bromide Methyl parathion Parathion Pentachlorphenol Triallate Trifluralin	Captan Carbaryl Chlordane Chloropyrifos DDT Dieldrin EDB EPTC Heptachlor Methyl bromide Methyl parathion Parathion Pentachlorphenol Triallate Trifluralin	Captan Carbaryl Chloropyrifos DDT Dieldrin EDB EPTC Heptachlor Methyl bromide Methyl parathion Parathion Pentachlorphenol Triallate Trifluralin	Captan Carbaryl Chloropyrifos DDT EDB Heptachlor Methyl bromide Methyl parathion Parathion Pentachlorphenol Triallate Trifluralin
$v = 0.01$ m/d	Chloropyrifos* Heptachlor Methyl bromide Methyl parathion Parathion Pentachlorphenol	Heptachlor Methyl bromide Methyl parathion Parathion Pentachlorphenol	Heptachlor Methyl bromide Methyl parathion Parathion Pentachlorphenol	Heptachlor Methyl bromide Methyl parathion Parathion Pentachlorphenol	Heptachlor Methyl bromide Methyl parathion Parathion Pentachlorphenol	Heptachlor Methyl bromide Parathion Pentachlorphenol
$v = 0.01$ m/d	Methyl bromide	Methyl bromide	Methyl bromide	Methyl bromide	Methyl bromide	Methyl bromide

* Chemical did not pass the dispersive screening model (17).

With the exception of carbaryl, all the highly volatile compounds ($K_H > 10^{-3}$) show lower than 1% of leached fractions below one meter depth at the low infiltration rate of 0.01 m/d in all soil textures. Among these highly volatile compounds, DDT, EDB, heptachlor, and trifluralin, are highly resistive to biochemical decay. Carbaryl ($K_H = 1.40 \times 10^{-3}$) does not satisfy the 1-m-depth-1% leaching criterion in silt clay loam and clay loam soils at $v = 0.01$ m/d; although it is short-lived ($\lambda = 22$ d). This may be attributed to a combination of lower K_H value relative to the other highly volatile compounds and relatively less adsorptive capacity due to a low K_{oc} value. Also, the lower organic carbon fractions f_{oc} in these two soil textures, as shown in Table 1, results in smaller predicted losses in the adsorbed phase, thereby more mass fraction available for leaching.

Note that the number of chemicals, which satisfy the leached fraction criterion of 1%, decreases from sand to clay loam texture where f_{oc} generally decreases according to the reported average values in Table 1. The average values of f_{oc} may not be indicative of the actual organic carbon fractions in real soils, as the coefficient of variation of f_{oc} for all soil textures (not shown in the table) is relatively high. For example, at $v = 0.01$ m/d, both convective–dispersive and purely convective models predict more than 1% leached fractions of dieldrin and EPTC in sandy clay loam, silt clay loam, and clay loam soils, where the average f_{oc} attains the lowest values among all soil textures. Those pesticides which do not show less than 1% leached fractions at depth $z = 1$ m in all soil textures at the considered infiltration rates are: atrazine, aldicarb, bromacil, carbofuran, cyanazine, 2,4-D, diazinon, diuron, and ethoprophos. Among these, atrazine, cyanazine, and simazine are commonly used in corn fileds.

At the assumed longitudinal dispersivity of 1 cm,

Table 4
Extension of Table 3 to other soil textures

	Silt clay loam	Clay loam	Sandy clay	Silt clay	Clay
$v = 0.01$ m/d	Captan Chloropyrifos DDT EDB Heptachlor Methyl bromide Methyl parathion Parathion Pentachlorphenol Triallate Trifluralin	Captan Chloropyrifos DDT EDB Heptachlor Methyl bromide Methyl parathion Parathion Pentachlorphenol *Trifluralin*	Captan Carbaryl Chloropyrifos DDT Dieldrin* EDB Heptachlor Methyl bromide Methyl parathion Parathion Pentachlorphenol Triallate Trifluralin	Captan Carbaryl Chloropyrifos DDT Dieldrin* EDB EPTC* Heptachlor Methyl bromide Methyl parathion Parathion Pentachlorphenol Triallate Trifluralin	Captan Carbaryl Chloropyrifos DDT EDB Heptachlor Methyl bromide Methyl parathion Parathion Pentachlorphenol Triallate Trifluralin
$v = 0.01$ m/d	Heptachlor Methyl bromide Pentachlorphenol	Heptachlor Methyl bromide Pentachlorphenol	Heptachlor Methyl bromide Methyl parathion Parathion Pentachlorphenol	Heptachlor Methyl bromide Methyl parathion Parathion Pentachlorphenol	Heptachlor Methyl bromide Methyl parathion Parathion Pentachlorphenol
$v = 0.01$ m/d	Methyl bromide Pentachlorphenol	Methyl bromide	Methyl bromide Parathion Pentachlorphenol	Heptachlor Methyl bromide Methyl parathion Parathion Pentachlorphenol	Heptachlor Methyl bromide Methyl parathion Parathion Pentachlorphenol

* Chemical did not pass the dispersive screening model (17).

both the convective–dispersive screening model (17) and the convective screening model (32) display similar screening results, except for the pesticides chloropyrifos, dieldrin, and EPTC (marked with $*$), which fail the screening test with the former. Table 5 contains chemicals that are, in addition to those shown in Tables 3 and 4, satisfy the 99% attenuation criterion for a hypothetical mobile–immobile phase soil with $\beta = 0.6$, $\alpha = 2.4\ \mathrm{d}^{-1}$ $(0.1\ \mathrm{h}^{-1})$ and $v = 0.01$ m/d. Half-life and f_{oc} are assumed to be similar in the mobile and immobile phases. Apparently, diffusive mass transfer and subsequent immobile-phase biochemical decay have no impact on the list of pesticides passing the screening test for soil textures sand and sandy clay loam soil textures. All pesticides in Table 5 that pass the test in other soil textures have moderately to high partition coefficient (Table 6), $K_{oc} > 0.23$. The larger the distribution coefficient, $K_d = K_{oc}\ f_{oc}$, the greater the predicted losses in the immobile phase. The diffusive loss parameter, ϕ, increases with greater values of K_{oc}, which leads to greater predicted losses in the immobile phase, as the

Table 5
List of additional chemicals satisfying 1% leaching criterion in hypothetical dual porosity soil, $\beta = 0.6$ and $\alpha = 2.4\ \mathrm{d}^{-1}$

	Sand	Loamy sand	Sandy loam	Silt loam	Loam	Sandy clay loam
$v = 0.01$ m/d		Linuron Phorate Prometryne	Linuron Phorate Prometryne	Linuron Phorate Prometryne	Chlordane Linuron Phorate Prometryne	

Table 6
Extension of Table 5 to other soil textures, $\beta = 0.6$ and $\alpha = 2.4\ d^{-1}$

	Silt clay loam	Clay loam	Sandy clay	Silt clay	Clay
$v = 0.01$ m/d	Carbaryl	Carbaryl Triallate	Dieldrin EPTC	Dieldrin EPTC	Dieldrin EPTC

leached fraction relationship (17) predicts. Chlordane is highly resistive to biochemical decay, $\lambda = 3500$ d, yet it satisfies the 1-m-depth-1% leaching criterion in loam soil texture because of its large K_{oc} value and the relatively large average organic carbon fraction in this soil texture, $f_{oc} = 0.003$. In this dual porosity soil, dieldrin and EPTC passed the screening test in all soil textures except at sandy clay loam, silt clay loam, and clay loam, where the reported average values of f_{oc} in Table 1 are the lowest.

5. Conclusions

Mass fraction models were developed for multiphase transport and fate of agricultural pollutants in two-region structured or aggregated soils under steady unsaturated flow conditions. Transport in the immobile phase was modeled with a first-order rate process, and the processes of vapor loss through soil surface (or volatilization) and absorption were particularly emphasized. Analytical expressions were developed for: (1) leached solute fractions; (2) vapor losses through soil surface; (3) transformation losses (biochemical and crop uptake) in the mobile phase; and (4) transformation losses in the immobile phase. Simulations based on the models demonstrated that leaching may be the net result of upward vapor-phase transport across soil–air interface relative to downward advective–dispersive transport, with lateral diffusion into stagnant-water soil regions acting as a moderating process. The model predicted that leached fraction of volatile compounds does not necessarily decrease monotonically with the relative residence time relative to half-life, but rather increase with this parameter relatively small values due to complex interactions among the physical and biochemical processes. Lateral diffusive transfer may be a significant process in reducing leaching, thereby the risk for ground-water pollution by pesticides. Longitudinal dispersion had a greater impact than lateral diffusive transfer on reducing vapor losses from soil surface; however, it showed increased potential for ground-water pollution. Vapor losses across the soil–air interface may reduce the risk for ground-water pollution, however, at the expense of increased potential for air pollution. Both leaching and volatilization losses decreased with increasing immobile–mobile phase coefficient, ϕ. Potential application of the modified leaching index was demonstrated by screening a selected group of pesticides according to a 99% attenuation criterion at depth 1 m in different soil textures under soil flux rates of 0.01, 0.1, 1.0 m/d. The screening results were largely dependent on the vapor-phase partition coefficient, K_H, and solute adsorption, including percentage of organic carbon fraction, f_{oc}. The effect of longitudinal dispersion was minimal at the chosen 1-m-depth-1% leached fraction criterion. More pesticides satisfied this leaching criterion in a hypothetical dual porosity soil. Screening models, which ignore lateral diffusive mass transfer, may yield an overly conservative screening list. Among the selected pesticides, Methyl Bromide satisfied the leaching criterion in all soil textures under the assumed infiltration rates. Atrazine, cyanazine, and simazine, which are commonly applied to corn plots, failed the screening test, among others, in all soil textures. Although the screening results were highly correlated with the reported average values of the organic carbon fraction in different soil textures, the latter were associated with relatively high values of the coefficient of variation. The screening results should therefore be cautiously interpreted in view of this fact, and a more reliable framework should factor in the uncertainty in this parameter and others. The presented analysis may have implications for the management of pesticides and the design of land treatment systems.

Acknowledgements

The US Environmental Protection Agency through its Office of Research and Development funded and managed the research described here through in-house efforts. The research was initially conducted at the Robert S. Kerr Environmental Research Center, Ada, Oklahoma. It has not been subjected to Agency review and therefore does not necessarily reflect the views of the Agency, and no official endorsement should be inferred. The authors thank Dr Barry and the anonymous reviewers whose comments improved the manuscript.

Appendix A. Derivation of leaching model

The Laplace transform of a function $f(z,t)$ is defined by:

$$\tilde{f}(z;p) = \int_0^\infty f(z,t)\, \mathrm{e}^{-pt}\mathrm{d}t \tag{A1}$$

The Laplace transforms of Eqs. (1), (2), (10a)–(10d), and (13) are given by

$$\begin{aligned} &pR_\mathrm{m}\tilde{C}_\mathrm{m}(z;p) - R_\mathrm{m}C_\mathrm{m}(z,0) + \beta R_\mathrm{im}p\tilde{C}_\mathrm{im}(z;p) \\ &\quad - \beta R_\mathrm{im}C_\mathrm{im}(z,0) + \beta k_\mathrm{im}R_\mathrm{im}\tilde{C}_\mathrm{im}(z;p) \\ &\quad = D_\mathrm{m}\frac{\mathrm{d}^2\tilde{C}_\mathrm{m}(z;p)}{\mathrm{d}z^2} - u\frac{d\tilde{C}_\mathrm{m}(z;p)}{\mathrm{d}z} \\ &\quad - k_\mathrm{m}(1+\mu)R_\mathrm{m}\tilde{C}_\mathrm{m}(z;p) \end{aligned} \tag{A2}$$

$$\beta R_\mathrm{im}p\tilde{C}_\mathrm{im}(z;p) - \beta R_\mathrm{im}C_\mathrm{im}(z,0) + \beta k_\mathrm{im}R_\mathrm{im}\tilde{C}_\mathrm{im}(z;p) = \alpha(\tilde{C}_\mathrm{m}(z;p) - \tilde{C}_\mathrm{im}(z;p)) \tag{A3}$$

$$\tilde{C}_\mathrm{m}(\infty,t) = \tilde{C}_\mathrm{im}(\infty,t) = 0 \tag{A4}$$

$$\tilde{F}_\mathrm{m}(0;p) = -\sigma\tilde{C}_\mathrm{m}(0;p) + M_\mathrm{o} + \frac{\sigma}{K_\mathrm{H}}\frac{C^*}{p} \tag{A5}$$

We first use Eq. (A3) to express $\tilde{C}_\mathrm{im}(z;p)$ in terms of $\tilde{C}_\mathrm{m}(z;p)$,

$$\tilde{C}_\mathrm{im}(z;p) = \frac{\alpha}{\beta R_\mathrm{im}(p+k_\mathrm{im})+\alpha}\tilde{C}_\mathrm{m}(z;p) \tag{A6}$$

Then, we substitute Eq. (A6) for $\tilde{C}_\mathrm{im}(z;p)$ into Eq. (A2) and use the initial condition (10a),

$$\begin{aligned} &\frac{\mathrm{d}^2\tilde{C}_\mathrm{m}(z;p)}{\mathrm{d}z^2} - \frac{u}{D_\mathrm{m}}\frac{\mathrm{d}\tilde{C}_\mathrm{m}(z;p)}{\mathrm{d}z} - \frac{R_\mathrm{m}}{D_\mathrm{m}}\left\{p + k_\mathrm{m}(1+\mu)\right. \\ &\quad \left. + \frac{1}{R_\mathrm{m}}\frac{\beta R_\mathrm{im}(p+k_\mathrm{im})\alpha}{\beta R_\mathrm{im}(p+k_\mathrm{im})+\alpha}\right\}\tilde{C}_\mathrm{m}(z;p) \\ &\quad = 0 \end{aligned} \tag{A7}$$

The solution of Eq. (A7) subject to boundary conditions (A4) and (A5) is obtained immediately,

$$\tilde{C}_\mathrm{m}(z;p) = \frac{1}{\sigma + \theta_\mathrm{m}D_\mathrm{m}m_2(p)}\left[M_\mathrm{o} + \frac{\sigma C^*}{K_\mathrm{H}}\frac{1}{p}\right]\mathrm{e}^{m_1(p)z} \tag{A8}$$

where

$$m_1(p) = (1/2)\left[u/D_\mathrm{m} - \sqrt{u^2/D_\mathrm{m}^2 + 4(R_\mathrm{m}/D_\mathrm{m})\left\{p + k_\mathrm{m}(1+\mu) + \frac{1}{R_\mathrm{m}}\frac{\beta R_\mathrm{im}(p+k_\mathrm{im})\alpha}{\beta R_\mathrm{im}(p+k_\mathrm{im})+\alpha}\right\}}\right] \tag{A9}$$

and

$$m_2(p) = (1/2)\left[u/D_\mathrm{m} + \sqrt{u^2/D_\mathrm{m}^2 + 4(R_\mathrm{m}/D_\mathrm{m})\left\{p + k_\mathrm{m}(1+\mu) + \frac{1}{R_\mathrm{m}}\frac{\beta R_\mathrm{im}(p+k_\mathrm{im})\alpha}{\beta R_\mathrm{im}(p+k_\mathrm{im})+\alpha}\right\}}\right] \tag{A10}$$

Since the Laplace transform of Eq. (11) is given by

$$\tilde{F}_\mathrm{m}(z;p) = -\theta_\mathrm{m}D_\mathrm{m}\frac{\mathrm{d}\tilde{C}_\mathrm{m}(z;p)}{\mathrm{d}z} + v\tilde{C}_\mathrm{m}(z;p) \tag{A11}$$

then the use of Eq. (A8) in Eq. (A11) yields

$$\tilde{F}_{\mathrm{m}}(z;p) = \left(M_{\mathrm{o}} + \frac{\sigma C^{*}}{K_{\mathrm{H}} p}\right) \frac{\theta_{\mathrm{m}} D_{\mathrm{m}} m_2(p)}{\sigma + \theta_{\mathrm{m}} D_{\mathrm{m}} m_2(p)} \mathrm{e}^{m_1(p) z} \tag{A12}$$

The limit in Eq. (16) can be evaluated using the well known identity:

$$f(\infty) = \lim_{p \to 0} \{ p \tilde{f}(p) \} \tag{A13}$$

Thus,

$$I_{\mathrm{l}}(z) = (1/M_{\mathrm{o}}) \lim_{p \to 0} \left\{ p \left(\frac{\tilde{F}_{\mathrm{m}}(z;p)}{p} \right) \right\} = (1/M_{\mathrm{o}}) \lim_{p \to 0} \tilde{F}_{\mathrm{m}}(z;p) \tag{A14}$$

In Eq. (A14), we used the fact that $\mathscr{L}\{ \int_0^t F_{\mathrm{m}}(z,\tau)\mathrm{d}\tau \} = \tilde{F}_{\mathrm{m}}(z;p)/p$, where $\mathscr{L}\{\ \}$ denotes the Laplace transform of the argument between parentheses. After setting $C^{*} = 0$ and substituting the right-hand side of Eq. (A12) for $\tilde{F}_{\mathrm{m}}(z;p)$ into Eq. (A14), and taking the limit $p \to 0$, one obtains Eq. (17).

References

Barry, D.A., Parker, J.C., 1987. Approximations for solute transport through porous media with flow transverse to layering. Transport Porous Media 2, 65–82.

Beltman, W.H.J., Boesten, J.J.T.I., van der Zee, S.E.A.T.M., 1995. Analytical modeling of pesticide transport from the soil surface to a drinking water well. J. Hydrol. 169, 209–228.

Campbell, G.S., 1974. A simple method for determining unsaturated conductivity from moisture retention data. Soil Sci. 117, 311–314.

Carsel, R.F., Mulkey, L.A., Lorber, M.N., Baskin, L.B., 1985. The Pesticide Root Zone Model (PRZM): A procedure for evaluating pesticide leaching threats to groundwater. Ecol Modell 30, 49–69.

Carsel, R.F., Parrish, R.S., Jones, R.L., Hansen, J.L., Lamb, R.L., 1988. Characterizing the uncertainty of pesticide leaching in agricultural soils. J. Contam. Hydrol. 2, 111–124.

Diaz, R.D., Loague, K., 2000. Regional-scale leaching assessments for Tenerife: effect of data uncertainties. J. Environ. Qual. 29, 835–847.

Freissinet, C., Vauclin, M., Elrich, M., 1999. Comparison of first-order analysis and fuzzy set approach for the evaluation of imprecision in a pesticide groundwater pollution screening model. J. Contam. Hydrol. 37, 21–43.

van Genuchten, M.T., Dalton, F.N., 1986. Models for simulating salt movement in aggregated field soils. Geoderma 38, 165–183.

van Genuchten, M.T., Wierenga, P.J., 1976. Mass transfer studies in sorbing porous media I. Analytical solutions. Soil Sci. Soc. Am. Proc. 40 (4), 473–480.

Goltz, M.N., Roberts, P.V., 1987. Using the method of moments to analyze three-dimensional diffusion-limited solute transport from temporal and spatial perspectives. Water Resour. Res. 23 (8), 1575–1585.

Griffioen, J.W., Barry, D.A., Parlange, J.-Y., 1998. Interpretation of the two-region model parameters. Water Resour. Res. 34 (3), 373–384.

Hantush, M.M., Mariño, M.A., 1998. Interlayer diffusive transfer and transport of contaminants in stratified formation. I: Theory. J. Hydrol. Engng, ASCE 3 (4), 232–240.

Hantush, M.M., Mariño, M.A., Islam, M.R., 2000. Models for leaching of pesticides in soils and groundwater. J. Hydrol. 227, 66–83.

Jarvis, N.J., 1994. MACRO version 3.1—Technical description and sample simulations. Reports and Dissertation No. 19, Department of Soil Science, Swedish University of Agricultural Sciences, Uppsala, Sweden, p. 51.

Jarvis, N.J., Jansson, P.E., Dik, P.E., Messing, I., 1991. Modelling water and solute transport in macroporous soil. I. Model description and sensitivity analysis. J. Soil Sci. 42, 59–70.

Jury, W.A., 1986. In: Hern, S.C., Melancon, S.M. (Eds.). Vadose Zone Modeling of Organic Pollutants, Chapter 11. Lewis Publishers, Chelsea, MI.

Jury, W.A., Farmer, W.J., Spencer, W.F., 1984. Behavior assessment model for trace organics in soil: II. Chemical Classification and Parameter Sensitivity. J. Environ. Qual. 13 (4), 567–572.

Jury, W.A., Gardner, W.R., Gardner, W.H., 1991. Soil Physics. Wiley, New York p. 328.

Khan, M.A., Liang, T., 1989. Mapping pesticide contamination potential. Environ. Mgmt 13, 233–242.

Kleveno, J.J., Loague, K., Green, R.E., 1992. Evaluation of a pesticide mobility index: impact of recharge variation and soil profile heterogeneity. J. Contam. Hydrol. 11, 83–99.

Laskowski, D.A., Goring, C.A.I., McCall, P.J., Swann, R.L., 1982. Terrest. Environ. In: Conway, R.A. (Ed.). Environmental Risk Analysis for Chemicals. Van Nostrand Reinhold, NY, pp. 198–240.

Li, E.A., Shanholtz, V.O., Carson, E.W., 1976. Estimating Saturated Hydraulic Conductivity and Capillary Potential at the Wetting Front. Department of Agricultural Engineering, Va. Polytech. Institute and State University, Blacksburg.

Li, L., Barry, D.A., Culligan-Hensley, P.J., Bajracharya, K., 1994. Mass transfer in soils with local stratification of hydraulic conductivity. Water Resour. Res. 30 (11), 2891–2900.

Loague, K., Green, R.E., Giambelluca, T.W., Liang, T.C., Yost, R.S., 1990. Impact of uncertainty in soil, climatic, and chemical information in a pesticide leaching assessment. J. Contam. Hydrol. 5, 171–194 see also page 405.

Loague, K., Bernknopf, R.L., Giambelluca, T.W., Green, R.E., 1995. The impact of data uncertainty upon regional scale leaching assessments of non-point source pollutants. Applications of GIS to the modeling of non-point source pollutants in the vadose

zone, ASA-CSSA-SSSA Bouyoucos Conference, Mission In, Riverside, CA.

Loague, K., Corwin, D.L., Ellsworth, T.R., 1998. The challenge of predicting nonpoint source pollution. J. Environ. Sci. Technol./ News, 130A–133A March.

Meeks, Y.J., Dean, J.D., 1990. Evaluating Ground-water vulnerability to pesticides. J. Water Resour. Plan. Mgmt 116 (5), 693–707.

Millington, R.J., Quirk, J.P., 1961. Permeability of porous solids. Trans. Faraday Soc. 57, 1200–1207.

Mulla, D.J., Perillo, C.A., Cogger, C.G., 1996. A site specific farm scale GIS approach for reducing ground water contamination by pesticides. J. Environ. Qual. 25 (3), 419–425.

Parker, J.C., Valocchi, A.J., 1986. Constraints on the validity of equilibrium and first-order kinetic transport models in structured soils. Water Resour. Res. 22 (3), 399–407.

Parlange, J.-Y., Starr, J.L., 1978. Dispersion in soil columns: effect of boundary conditions and irreversible reactions. Soil Sci. Soc. Am. J. 42, 15–18.

Rao, P.S.C., Hornsby, A.G., Jessup, R.E., 1985. Indices for ranking the potential for pesticide contamination of groundwater. Proc. Soil Crop Sci. Soc. Fla. 44, 1–8.

Rawls, W.J., 1983. Estimating soil bulk density from particle size analysis and organic matter content. Soil Sci. 135 (2), 123–125.

Shukla, S., Mostaghimi, S., Shanholt, V.O., Collins, M.C., Ross, B.B., 2000. A county-level assessment of ground water contamination by pesticides. Ground Water Monitor. & Remed. 20 (1), 104–119.

Wagenet, R.J., Hutson, J.L., 1989. LEACHM: A Finite Difference Model for Simulating Water, Salt and Pesticide Movement in the Plant Root Zone. , Continuum. Version 2.0, vol. 2. New York State Water Resource Institute, Cornell University, Ithaca, NY.

Wagenet, R.J., Rao, P.S.C., 1990. Modeling pesticide fate in soils. In: Cheng, H.H. (Ed.). Pesticides in the Soil Environment: Processes, Impacts, and Modeling. SSSA Book Series, vol. 2. pp. 351–399.

van der Werf, H.M.G., 1996. Assessing the impact of pesticides on the environment. Agric., Ecosyst. Environ. 60, 81–96.

Yates, S.R., Papiernik, S.K., Gao, F., Gan, J., 2000. Analytical solutions for the transport of volatile organic chemicals in unsaturated layered system. Water Resour. Res. 36 (8), 1993–2000.

van der Zee, S.E.A.T.M., Boesten, J.J.T.I., 1991. Effects of soil heterogeneity on pesticide leaching to groundwater. Water Resour. Res. 27 (12), 3051–3063.